A microfluidic approach for hemoglobin detection in whole blood

Nikita Taparia,[1] Kimsey C. Platten,[1] Kristin B. Anderson,[1]
and Nathan J. Sniadecki[1,2,3,a]
[1]*Mechanical Engineering, University of Washington, Seattle, WA 98105, USA*
[2]*Bioengineering, University of Washington, Seattle, WA 98105, USA*
[3]*Institute for Stem Cell and Regenerative Medicine, University of Washington, Seattle, WA 98105, USA*

(Received 21 July 2017; accepted 5 September 2017; published online 3 October 2017)

Diagnosis of anemia relies on the detection of hemoglobin levels in a blood sample. Conventional blood analyzers are not readily available in most low-resource regions where anemia is prevalent, so detection methods that are low-cost and point-of-care are needed. Here, we present a microfluidic approach to measure hemoglobin concentration in a sample of whole blood. Unlike conventional approaches, our microfluidic approach does not require hemolysis. We detect the level of hemoglobin in a blood sample optically by illuminating the blood in a microfluidic channel at a peak wavelength of 540 nm and measuring its absorbance using a CMOS sensor coupled with a lens to magnify the image onto the detector. We compare measurements in microchannels with channel heights of 50 and 115 μm and found the channel with the 50 μm height provided a better range of detection. Since we use whole blood and not lysed blood, we fit our data to an absorption model that includes optical scattering in order to obtain a calibration curve for our system. Based on this calibration curve and data collected, we can measure hemoglobin concentration within 1 g/dL for severe cases of anemia. In addition, we measured optical density for blood flowing at a shear rate of 500 s^{-1} and observed it did not affect the nonlinear model. With this method, we provide an approach that uses microfluidic detection of hemoglobin levels that can be integrated with other microfluidic approaches for blood analysis.
[http://dx.doi.org/10.1063/1.4997185]

I. INTRODUCTION

Hemoglobin is a protein within red blood cells that is responsible for oxygen transportation. When hemoglobin is either absent, flawed, or impaired, the reduced levels of oxygen in the blood leads to dizziness, fatigue, shortness of breath, and abnormal heart rate.[1,2] Low hemoglobin concentration is diagnosed as anemia, which is caused by more than seventeen different diseases, mainly iron deficiency, hemoglobinopathy, and malaria.[3–6] The World Health Organization recognizes anemia as a global health problem, affecting a quarter of global population and having prevalence in young children and women.[1,2,7–9] Thus, it is important to measure and monitor hemoglobin in these high-risk subpopulations.

Laboratory analysis of hemoglobin concentration is measured with a hematology analyzer as part of a complete blood count (CBC) panel. Hematology analyzers take advantage of the optical absorption of hemoglobin at a wavelength of 540 nm in order to detect its concentration. Specifically, red blood cells in a sample are lysed to release their hemoglobin proteins. Then, hemoglobin is chemically converted to a stable form, cyanmethemoglobin, for optical detection.[10] From

[a]Author to whom correspondence should be addressed. Electronic mail: nsniadec@uw.edu

Beer-Lambert law, the light absorbance at 540 nm is proportional to the hemoglobin concentration in a sample.[11,12] While this method is accurate and reliable, it is used scarcely in resource-poor regions, which coincidentally have the highest cases of anemia.[1]

To advance the technology beyond its current capabilities, research has shifted focus towards methods for hemoglobin detection that are portable and affordable. These new detection methods still take advantage of the optical absorption of hemoglobin, but differ in how they process a blood sample. For example, a portable hemoglobinometer measures light transmission through a chemical-laced cuvette of blood.[13] This approach has been replicated in platform based on a smartphone, in which the built-in camera sensor detects light transmission through a cuvette or microfluidic device.[14,15] Alternatively, some methods use paper to absorb treated blood prior to performing a colorimetric analysis.[16,17] In addition, a centrifugal microfluidics platform uses rigorous mixing of whole blood and chemicals prior to optical readouts.[18] While these techniques have established a capability to measure hemoglobin, they currently rely on the hemolysis of whole blood.

Hemolysis is favorable for accurate hemoglobin measurements, but it prevents the potential integration with existing or future blood diagnostic platforms. Specifically, there have been separate efforts to diagnose blood diseases in microfluidic assays by measuring the deformability of red blood cells.[19,20] These measurements allow one to determine the presence of malaria or sickle-cell disease, which can be the underlying cause of anemia.[8] While high-risk subpopulations have been identified from hemoglobin concentration measurements, global health communities acknowledge that the reduction of anemia burden requires more detailed epidemiology of the disease because it can lead to targeted treatment.[8,21] Avoiding the process of hemolysis would be a step towards an integrated diagnostic platform for anemia and other blood-related conditions.

Here, we present a method to measure hemoglobin concentration with whole blood in a microfluidic device. Typically, the light transmission through lysed blood can determine the hemoglobin concentration solely based on the light absorption. Here, because of the use of whole blood, light transmission can still determine the hemoglobin concentration, but it must also account for light scattering. Using this system, we explore the effect of path length and flow rate within the microfluidic device to optimize the detection of hemoglobin for different hematocrit levels. The findings of this study serve as a preliminary step towards a more integrated approach for anemia surveillance.

II. MATERIALS AND METHODS

A. Blood handling and sample preparation

Blood collection and a complete blood count (CBC) panel were ordered for each human subject under an institutional review board (IRB)-approved protocol from University of Washington. Blood samples were collected in sodium citrate tubes (0.109 M/3.2%, 2.7 mL, BD Vacutainer, Becton, Dickinson and Company). The CBC panel provided the total hematocrit and hemoglobin level for each donor. In order to adjust the hematocrit levels for analysis, we diluted a portion of a blood sample with calcium free Tyrode buffer (10 mM HEPES, 138 mM NaCl, 5.5 mM glucose, 12 mM $NaHCO_3$, 0.36 mM Na_2HPO_4, 2.9 mM KCl, 0.4 mM $MgCl_2$ in DI H_2O). Each dilution was loaded into a 3-mL syringe (BD Scientific) and kept on an orbital rocker prior to experiments to prevent any cell sedimentation that would affect the measurements.

B. Fabrication of microfluidic device

Photolithography of SU-8 photoresist or deep reactive ion etching was used to create two silicon masters for the microfluidic devices with channel heights of 50 and 115 μm, respectively (Figure S1(a) of the supplementary material). Specifically, these channels had rectangular cross-sectional areas, in which the first device had a length, width, and height of 3 cm x 200 μm x 50 μm and the second device had 1 cm x 1 mm x 115 μm. Using soft lithography, polydimethylsiloxane (PDMS) (Sylgard 184, Dow Corning) was made with a 10:1 base to curing agent ratio, mixed for 5 minutes, degassed for 20 minutes, and then poured over the master. The PDMS and master were placed in an oven for 10 minutes at 110 °C to form a negative mold (Figure S1(b) of the supplementary material). This negative mold was exposed to plasma (Plasma Prep II, Structure Probe, Inc.) for 10 seconds. Afterwards, the molds were treated with tridecafluoroctyltrichlorosilane (United Chemical Technologies) under

vacuum pressure in a desiccator for 2 hours. Uncured PDMS was degassed, poured onto the mold, cast on a microscope slide, and cured at 110 °C for 24 hours (Figure S1(c) of the supplementary material). The mold was peeled away from the glass and PDMS channels remained to form the bottom layer (Figure S1(d) of the supplementary material). The top layer for the microchannel was made using a custom aluminum mold with pegs to insert the silicone tubing (0.040 inch ID/ 0.085 inch OD, HelixMark) for the inlet and outlet port. Degassed 10:1 PDMS was poured into the preheated aluminum mold and cured for 110 °C for 1 hour (Figure S1(e) of the supplementary material). The top layer and bottom layer were plasma treated for 10 seconds and then aligned together to create a water-tight seal between the two layers (Figure S1(f) of the supplementary material).

C. Optical apparatus

A miniature microscope was constructed to measure the transmitted intensity of light (Fig. 1(a)). The sample was illuminated with a white LED (sr-06-wn300, LuxeonStar) paired with a TRITC

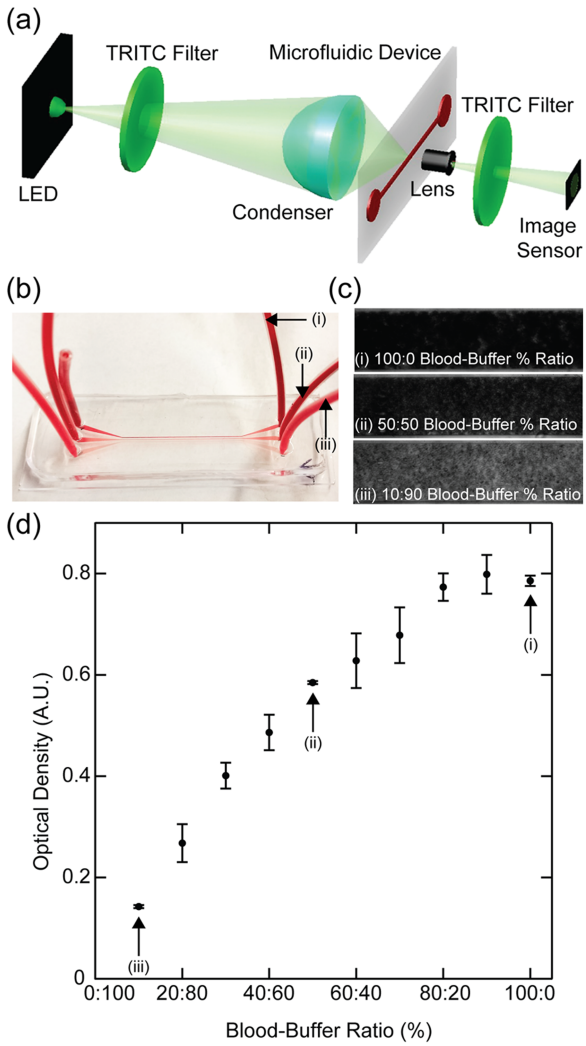

FIG. 1. Experimental method to detect optical density in whole blood. (a) A light emitting diode and TRITC excitation filter (532-552 nm) coupled with an aspheric condenser illuminates a microfluidic channel with green light. This green light goes through a lens and a second TRITC excitation filter and the final image is captured via the image sensor. (b) A microchannel is filled with different blood to buffer percentage ratios, (i) 100:0, (ii) 50:50, (iii) 10:90. (c) The microchannel is imaged with and without blood to determine light intensity before and after the blood. (d) Optical density is obtained by measuring the transmission of light before and after blood entered the microchannel. The optical density of a sample was changed by diluting the blood with Tyrode Buffer.

excitation filter (mf542-20, Thorlabs), which has a bandwidth of 532-552 nm. The light was focused onto a microfluidic channel with an aspheric condenser (acl2520, Thorlabs). Transmitted light through the microfluidic channel was captured through a board lens (tbl 2.8 5mp, ImagingSource) whose orientation was reversed to magnify the image of the channel. Another TRITC excitation filter was placed in front of the USB powered CMOS camera board (SMN-B050-U, Mightex). A motorized micrometer (Z812B, Thorlabs) was used to adjust the focus to the bottom of the channel for accurate measurements of optical transmission through the full path length. Images were taken at the same exposure time and the LED maintained the same current.

D. Experimental procedure

For each experiment, whole blood was diluted with Tyrode buffer and gently rocked prior to its injection into a microfluidic channel. The hematocrit and hemoglobin levels for these dilutions were calculated based on the original CBC panel for each donor. Reference images were taken to get the initial intensity of light transmission prior to blood within the channel. After the reference images were taken, blood was injected into the channel (Figure 1(b)). After blood entered the channel, data images were taken (Figure 1(c)).

To determine the optimal channel depth for optical density measurements, two different channel heights, 50 and 115 μm, were compared. Blood for different hematocrit levels was pipetted into the channel and images were taken. Hematocrit levels were tested at least two times for four subjects. In addition, extra subjects were tested to baseline measurements and improve our fitted model.

To determine the effect of shear rate on the measurement of optical density of whole blood, a syringe pump (Model PHD Ultra 4400, Harvard Apparatus) regulated flow through the channel with a depth of 50 μm. Images were taken before blood entered the device to record the unobstructed light transmission through the channel. Then, images were taken as blood flowed at a shear rate of 500 s^{-1}, through the channel. Immediately after the blood came to a halt in the channel, images of the static blood were taken. Hematocrit levels were tested at least two times for four subjects.

E. Image analysis

Ten reference images were taken before blood entered the channel and ten data images were taken after blood entered the channel. Images were imported as a stack in ImageJ. A region of interest within the channel was chosen and the average intensity was measured for each frame. The average value for the corresponding frames represented the intensity before and after blood entered the channel, respectively. These intensity measurements were used to determine optical density.

F. Analytical model for light absorbance

Current methods of hemoglobin detection require the lysis of red blood cells and chemical conversion of hemoglobin into a stable color product. From this procedure, a linear relationship arises between hemoglobin concentration and light absorption at a wavelength of 540 nm, otherwise known as Beer-Lambert's law. However, there is a deviation from this linear relationship if the red blood cells stay intact because their membrane scatters the light. Thus, any method that uses whole blood must account for light scatter to obtain accurate measurements of hemoglobin concentration.

For this study, we used a generalized model from Steinke and Shephard to measure hemoglobin concentration in whole blood.[22] The advantage of this model is the use of optical properties of blood such as the absorption and scattering coefficient (μ_a and μ_s) and fractional hematocrit (H).

Optical density, a unitless quantity, is typically used to describe light transmission through a medium. Optical density (OD) has a logarithmic relationship with the transmittance (T), as described by,

$$OD = -\log_{10} T. \tag{1}$$

The transmittance is represented as

$$T = e^{-\Sigma d}, \tag{2}$$

where d is the path length. The characteristic length (Σ) describes the macroscopic change of light flux due to whole blood and is the sum of an absorption and scattering component, represented as

$$\Sigma = \Sigma_a + \Sigma_s. \tag{3}$$

The macroscopic absorption and scattering characteristic lengths, Σ_a and Σ_s, can be defined in terms of the microscopic absorption and scattering cross section area for a single red blood cells. Steinke and Shephard[22] define these relationships as

$$\Sigma_a = \frac{\sigma_a}{V} H \tag{4}$$

$$\Sigma_s = \frac{\sigma_s}{V} H\,(1-H)\,(1.4-H)\,, \tag{5}$$

where σ_a is the absorption cross section area, σ_s is the scattering cross section area, V is the volume of the red blood cell, and H is the fractional hematocrit. The coefficient, μ, for either absorption or scattering, is defined as the total cross-sectional area per unit volume. Thus, the final form of characteristic length that describes the change in light flux due to whole blood is

$$\Sigma = \mu_a H + \mu_s H\,(1-H)\,(1.4-H)\,, \tag{6}$$

where μ_a and μ_s are absorption and scattering coefficients, respectively.

Using equations (1), (2) and (6) and applying a scale factor (k), we obtain a final expression given by

$$OD = k(\mu_a H + \mu_s H\,(1-H)\,(1.4-H))d. \tag{7}$$

Here, the absorption and scattering coefficients are $\mu_a = 0.0743$, and $\mu_s = 0.823$, respectively, based on a previous study that used a wavelength in our range of interest, 532-552 nm.[23] It is also known that these coefficients change relative to the shear rate on the red blood cells.[24] For our optical apparatus, we assumed coefficients related to static conditions and found the data fit well when $k = 0.15457$, which we will present in the Results section. Since hemoglobin and hematocrit have a linear dependence with each other, we can transform this model to predict hemoglobin concentration as well.[11] A Bland-Altman plot can identify the bias and limits of agreement based on the comparison of these model predictions to the actual measurement from the CBC panel.

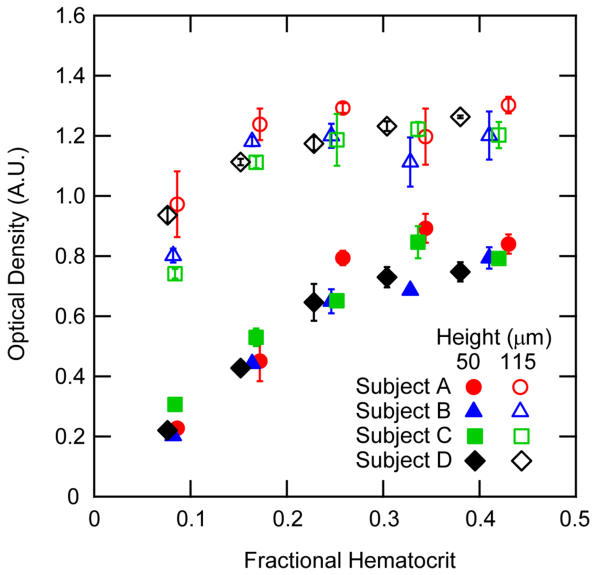

FIG. 2. Microchannel height affects the detection approach. Optical density was measured in microfluidic channels with heights 50 μm (filled marker) or 115 μm (empty markers) for five different dilutions of whole blood, which we report by fractional hematocrit levels. It should be noted, the lowest hematocrit level for subject A in the 50 μm channel (red, filled circle marker) was the only data point with one repetition.

III. RESULTS

A. Simulation of anemia

Anemia diagnosis is based on a lower level of hematocrit, or by equivalence, a lower level of hemoglobin concentration. To simulate a state of anemia in a blood sample, it was diluted with Tyrode buffer to change its hematocrit levels. As the percentage of blood changed, there was a monotonic change in optical density (Figure 1(d)). However, the optical density did not increase linearly for blood dilutions higher than 40%. As blood dilution approaches 80%, there is a saturation

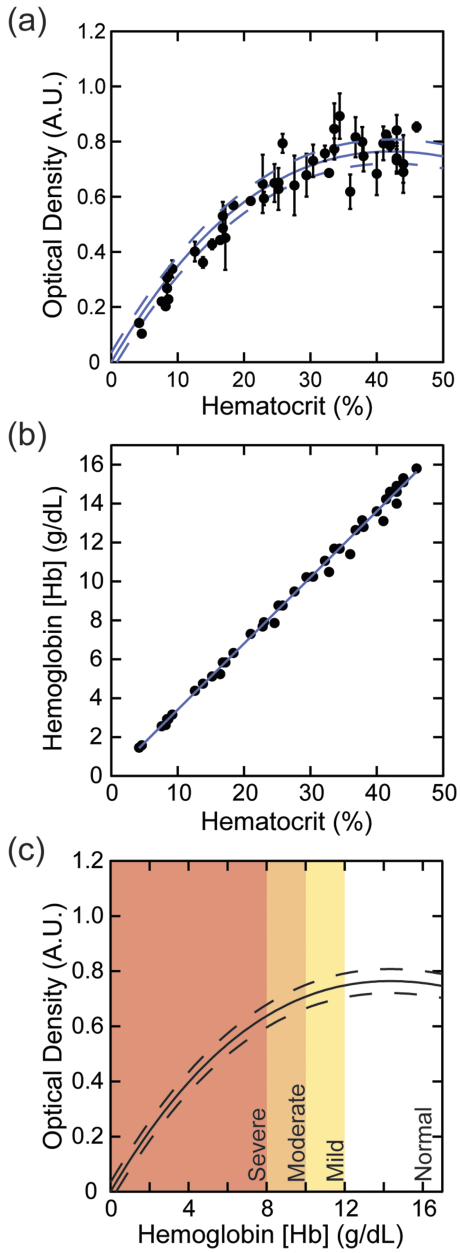

FIG. 3. A nonlinear model was fitted to the data. (a) A model (solid line) given by equation 7 that uses the optical properties of the blood, hematocrit level, and path length was fitted to the data. The 95% confidence interval for the model are indicated by dashed lines. (b) A linear relationship between hemoglobin and hematocrit was verified. (c) Afterwards, the model was linearly transformed to measure hemoglobin based on optical density measurements. Based on the designation from the World Health Organization, different severity regimes for anemia are designated.

with optical density, making it difficult to associate a measurement with an optical density reading. Thus, the saturation in the optical density at higher levels of hematocrit define the upper limits of our detection.

B. Variations in path length

Because Beer-Lambert's law indicated a dependence on path length, it was important to test its effect with our optical detection apparatus. The effect of path length on optical density measurements was tested for two different path lengths: 50 and 115 μm. As indicated by the change of hematocrit levels, there was a monotonic change in optical density, which defined a nonlinear relationship (Figure 2). For a path length of 115 μm, changes in optical density diminished above a fractional hematocrit level of 0.15, which indicates there would be difficulty in diagnosing moderate or severe cases of anemia. In contrast, it was possible to detect changes in fractional hematocrit below 0.30 in a microchannel with a path length of 50 μm. This result indicates the optical detection of anemia should be possible for the moderate and severe cases of anemia. From this, we concluded a microfluidic device with the 50 μm channel height provided a better range of detection than the 115 μm channel height.

C. Fit to model and detection range

We used the data for the 50 μm channel height to obtain a fit to equation 7 (Figure 3(a)). For the scaling parameter found, the overall fit had a root mean square error of 0.0135 and a coefficient of determination of 0.847, where the largest variance occurs in the region of higher hematocrit. Because the model originally considers fractional hematocrit, we confirmed that there was a linear relationship between hemoglobin concentration and hematocrit (Figure 3(b)), which has been reported previously.[25] With this relationship, we could apply the model for hemoglobin concentration to the experimental data (Figure 3(c)). Based on the width of the 95% confidence interval, estimations can be made about the upper limits of this detection method. Specifically, as the optical density saturates, the width of the 95% confidence bands increase, which indicates that there is less accuracy in the measurement of hemoglobin.

For a more definitive determination of the range of hemoglobin detection, a Bland-Altman plot was constructed to compare the model prediction to the original measurement from a complete blood count (Figure 4).[26] The model and optical density measurements were used to determine the predicted

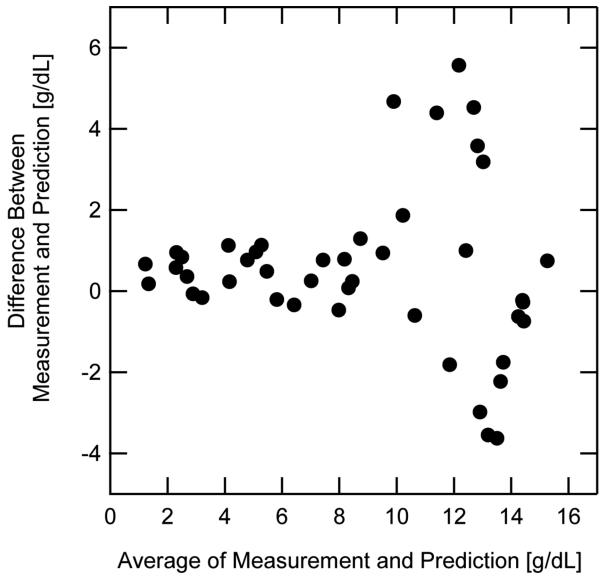

FIG. 4. A Bland-Altman plot identifies the limits of agreement for the bias between the actual measurement of hemoglobin and our device prediction to increase from severe anemia to normal ranges of hemoglobin concentration. The nonlinear model was used to predict the hemoglobin level based on the measurements of the optical density. This prediction was compared to the original measurement of hemoglobin acquired from the complete blood count panel.

TABLE I. Results of the Bland-Altman assessment for each anemia severity range.

Anemia Severity	Range (g/dL)	Bias (g/dL)	Limits (g/dL)
Severe	0-8	0.425	±1.005
Moderate	8-10	1.336	±3.394
Mild	10-12	0.962	±5.509
Normal	>12	0.023	±6.444

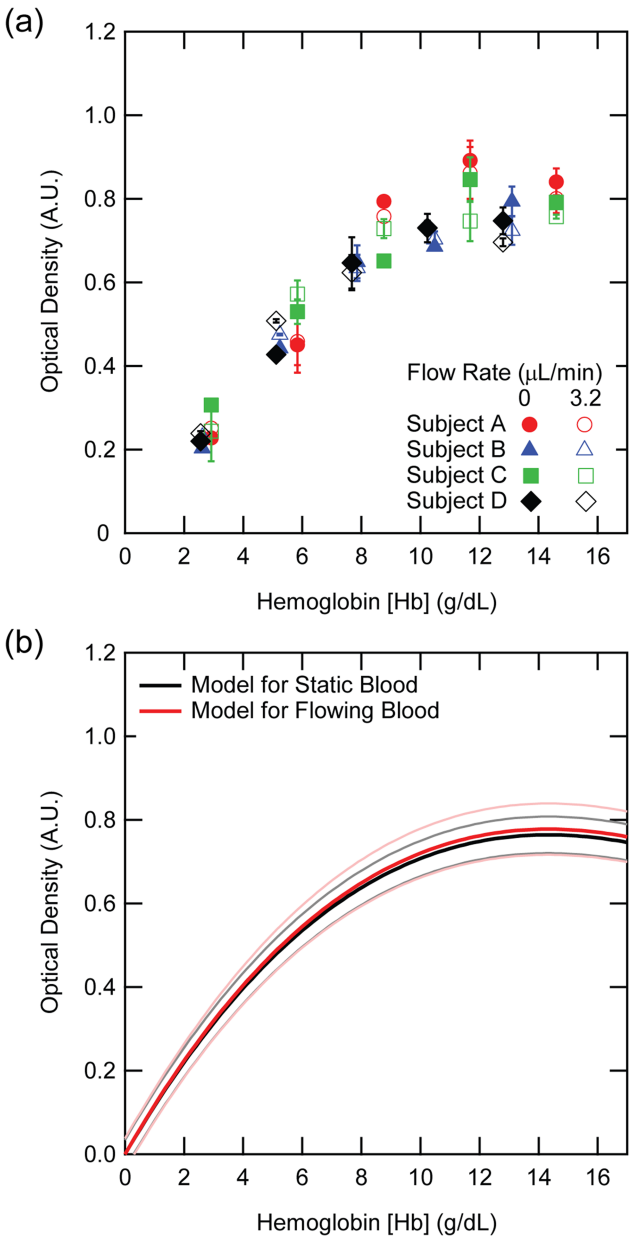

FIG. 5. Flow rate did not change the hemoglobin predictions significantly. (a) The optical density for four donors' blood, subject to static and flowing blood are plotted for five different levels of hemoglobin. The flow rate of 3.2 μL/min is equivalent to a shear flow of 500 s^{-1} in the 50 μm channel. It should be noted, the lowest hemoglobin level for subject A in the static measurement (red, filled circle marker) was the only data point with one repetition. (b) Using the optical density data from the flowing blood measurements, a separate calibration model and its 95% confidence interval was found (red) and compared to the original static calibration model (black).

hemoglobin concentration. The bias and limits of agreement was found for severe, moderate, and mild anemia, defined by the World Health Organization (Table I). Based on the Bland-Altman assessment, our technique can determine severe and moderate anemia with higher certainty in whole blood. The limits of agreement for our technique increases to 6.444 g/dL for normal hemoglobin ranges, which indicates this technique is unlikely to give false negative anemia diagnosis.

D. Variations in flow rate

To test the effect of flow rate, the optical density was measured a shear rate of 500 s^{-1} in the microfluidic channel with a path length of 50 μm in comparison to static flow (Figure 5(a)). Specifically, four donors with known hemoglobin levels were tested under flow and compared to the static measurements of optical density for several dilutions. Our motivation to test the effect of shear on the optical density of whole blood was due to a previous study that reported the scattering coefficient of whole blood to be different in static conditions and at shear rates of 200 s^{-1}. As seen in equation 7, a difference in scattering coefficient would have an effect on the measurement of optical density. However, in our technique, a separate model fit was found for the blood under flow and compared to the static flow measurements (Figure 5(b)). There is a direct overlap between the fit specifically in the anemic regime and this overlap deviates for measurements in the normal hemoglobin region. In addition, the fit line and its confidence band for the flow measurements falls within the confidence band of the static measurements. Thus, the model found in the static conditions can still determine severe and moderate anemia for flowing blood in a microfluidic setting.

IV. DISCUSSION

Anemia is a global health problem, but new affordable, portable detection methods can provide a means to diagnose the disease in low-resource regions. We developed an approach that uses simple optics and a microfluidic card to measure hemoglobin concentration without the need for hemolysis. We found a path length to measure hemoglobin before the changes in optical density became too small to distinguish between hemoglobin concentration. With this specific path length, our technique was able to determine hemoglobin concentration for hematocrit conditions that mimic severe and moderate anemia in static whole blood. This model also held true for flow conditions that have previously demonstrated a shift in the scattering properties of red blood cells.

Path length is known to affect the optical transmission of light, theoretically and experimentally. Therefore, we tested path length in two different microfluidic devices with channel heights of 50 and 115 μm. In general, optical density increased in proportion to hematocrit levels until the measurable change in light transmission became too small to distinguish between hematocrit levels. This saturation effect in the optical density occurs because of the scatter from red blood cells as opposed to light absorption of hemoglobin from hemolyzed blood. As a result, the range of detection only includes the region with a positive slope relationship. A previous study found the initial slope of this detectable region changed with path length, but the range of detection remained the same.[27] However, these studies were done with red or infrared spectra lasers and explored thicker path lengths. In this study, we found a path length of 50 μm was preferable primarily because the positive slope in optical density extended through most of the anemic range prior to saturation.

The data in this study was fitted to a cubic model, which includes parameters for the optical properties of blood, hematocrit level, and path length. Using our model, we found our predictions for hemoglobin concentration in whole blood had a bias of 0.42 ± 1.01 g/dL for a case of severe anemia. In comparison, a paper-based method could detect hemoglobin from lysed blood for all ranges with a bias of 0.62 ± 1.24 g/dL.[17] Additionally, a microcuvette method with cell phone detection had a bias of 0.036 ± 0.585 g/dL for mild anemia and normal conditions.[14] While our method increases uncertainty towards normal conditions, it is more likely to give a false positive at a higher concentration than a false negative at a lower range.

More importantly, flow rate did not change the predicted model. In previous studies, it was found that an increase in shear rate changed the scattering and absorption properties of whole blood.[24] Specifically, for a shear rate from 0 to 200 s^{-1}, there was a decrease in scattering coefficient in a

97 and 116 μm cuvette, respectively, and this was attributed to the Fahraeus effect. The Fahraeus effect corresponds to a change in hematocrit in flow with respect to tube diameter.[28] However here, we found a shear rate of 500 s^{-1} did not alter the fitted model for static conditions. Therefore, this technique to measure the hemoglobin levels can run parallel to other microfluidic tests that require flowing intact blood cells.

Currently, methods to measure hemoglobin concentration require red blood cell lysis through chemical reactions. Hemolysis eliminates scattering effects from the red blood cell and this leads to a linear relationship between optical density and hemoglobin concentration, solely dependent on the absorption coefficient. Thus, while lysis is advantageous for absolute measurements of hemoglobin, whole blood eliminates some of the blood handling required and allows for further testing of the same sample in a microfluidic setting. The advantage of microfluidics is to create multiple regions for different testing. As noted by Kassembaum, there are three major reasons for anemia: iron deficiency, hemoglobinopathy, and malaria.[8] The ability to detect not just the concentration of hemoglobin, but also the etiology will help determine the prevalence of anemia and its cofactors in different demographics. Currently, some of these microfluidic devices for malaria detection use red blood cell deformability or electrophoresis and therefore, they require intact whole blood.[19,20,29] Thus, a microfluidic device that can detect malaria and severe anemia can provide more detailed information in one test. With our proposed method to determine the severity of anemia, there is potential to combine these measurement capabilities into one diagnostic platform for anemia surveillance.

V. CONCLUSION

Anemia is a global health problem that affects a quarter of the world's population and is a result of many different factors including but not limited to iron deficiency, malaria, and genetic disorders. To promote the continued diagnosis and reporting of anemia in areas of highest prevalence, there has been a rise of point-of-care devices that focus on the measurement of hemoglobin concentration. While these solutions provide accurate measurement of hemoglobin concentration, global health communities have called for a technique that can help differentiate the cause of anemia in these subpopulations. In this paper, we presented a method to measure hemoglobin in a microfluidic device from whole blood. This approach can detect moderate and severe anemia with small volumes of whole blood. Because of the use of whole blood in a microfluidic setting, many other microfluidic blood diagnostic platforms that screen for causes of anemia such as malaria, can easily adapt our methodology to measure hemoglobin. An integrated diagnostic tool will aid the global health community in their continued surveillance of anemia and its etiology in high risk subpopulations.

SUPPLEMENTARY MATERIAL

See supplementary material for the fabrication process of the microfluidic channel devices.

ACKNOWLEDGMENTS

This work was supported by the Department of Education GAANN Fellowship and the National Science Foundation Grant CMMI-1402673.

[1] Y. Balarajan *et al.*, "Anaemia in low-income and middle-income countries," Lancet **378**(9809), 2123–2135 (2011).
[2] E. McLean *et al.*, "Worldwide prevalence of anaemia, WHO Vitamin and Mineral Nutrition Information System, 1993-2005," Public Health Nutrition **12**(4), 444–454 (2009).
[3] C. Menendez, A. F. Fleming, and P. L. Alonso, "Malaria-related anaemia," Parasitology Today **16**(11), 469–476 (2000).
[4] B. T. Kadima *et al.*, "High rate of sickle cell anaemia in Sub-Saharan Africa underlines the need to screen all children with severe anaemia for the disease," Acta Paediatrica **104**(12), 1269–1273 (2015).
[5] F. Kateera *et al.*, "Malaria, anaemia and under-nutrition: Three frequently co-existing conditions among preschool children in rural Rwanda," Malaria Journal **14** (2015).
[6] K. M. Nair *et al.*, "Characterisation of anaemia and associated factors among infants and pre-schoolers from rural India," Public Health Nutrition **19**(5), 861–871 (2016).
[7] G. A. Stevens *et al.*, "Global, regional, and national trends in haemoglobin concentration and prevalence of total and severe anaemia in children and pregnant and non-pregnant women for 1995-2011: A systematic analysis of population-representative data," Lancet Global Health **1**(1), E16–E25 (2013).

[8] N. J. Kassebaum *et al.*, "A systematic analysis of global anemia burden from 1990 to 2010," Blood **123**(5), 615–624 (2014).
[9] S. R. Pasricha, "Anemia: A comprehensive global estimate," Blood **123**(5), 611–612 (2014).
[10] D. L. Drabkin and J. H. Austin, "Spectrophotometric studies II. Preparations from washed blood cells; nitric oxide hemoglobin and sulfhemoglobin," Journal of Biological Chemistry **112**(1), 51–65 (1935).
[11] B. J. Bain, *Blood Cells: A Practical Guide* 2015 (Wiley-Blackwell).
[12] S. M. Lewis *et al.*, "Lauryl sulphate haemoglobin: A non-hazardous substitute for HiCN in haemoglobinometry," Clin Lab Haematol **13**(3), 279–290 (1991).
[13] M. Munoz *et al.*, "Utility of point-of-care haemoglobin measurement in the HemoCue-B haemoglobin for the initial diagnosis of anaemia," Clin Lab Haematol **27**(2), 99–104 (2005).
[14] H. Y. Zhu *et al.*, "Cost-effective and rapid blood analysis on a cell-phone," Lab on a Chip **13**(7), 1282–1288 (2013).
[15] T. Guo *et al.*, "Smartphone dongle for simultaneous measurement of hemoglobin concentration and detection of HIV antibodies," Lab on a Chip **15**(17), 3514–20 (2015).
[16] M. Bond *et al.*, "Chromatography paper as a low-cost medium for accurate spectrophotometric assessment of blood hemoglobin concentration," Lab on a Chip **13**(12), 2381–2388 (2013).
[17] X. X. Yang *et al.*, "Simple paper-based test for measuring blood hemoglobin concentration in resource-limited settings," Clinical Chemistry **59**(10), 1506–1513 (2013).
[18] J. Steigert *et al.*, "Direct hemoglobin measurement on a centrifugal microfluidic platform for point-of-care diagnostics," Sensors and Actuators A-Physical **130**, 228–233 (2006).
[19] H. W. Hou *et al.*, "Deformability based cell margination—A simple microfluidic design for malaria-infected erythrocyte separation," Lab on a Chip **10**(19), 2605–2613 (2010).
[20] J. P. Shelby *et al.*, "A microfluidic model for single-cell capillary obstruction by Plasmodium falciparum infected erythrocytes," Proceedings of the National Academy of Sciences of the United States of America **100**(25), 14618–14622 (2003).
[21] N. J. Kassebaum, "The global burden of anemia," Hematol Oncol Clin North Am **30**(2), 247–308 (2016).
[22] J. M. Steinke and A. P. Shepherd, "Diffusion-model of the optical absorbance of whole-blood," Journal of the Optical Society of America A-Optics Image Science and Vision **5**(6), 813–822 (1988).
[23] M. Hammer *et al.*, "Single scattering by red blood cells," Applied Optics **37**(31), 7410–7418 (1998).
[24] M. Friebel *et al.*, "Influence of shear rate on the optical properties of human blood in the spectral range 250 to 1100 nm," Journal of Biomedical Optics **12**(5) (2007).
[25] H. H. Billett, "Hemoglobin and hematocrit," in *Clinical Methods: The History, Physical, and Laboratory Examinations*, edited by H. K. Walker, W. D. Hall, and J. W. Hurst (Butterworth Publishers, Boston, 1990).
[26] J. M. Bland and D. G. Altman, "Statistical methods for assessing agreement between two methods of clinical measurement," Lancet **1**(8476), 307–310 (1986).
[27] R. J. Zdrojkowski and N. R. Pisharoty, "Optical transmission and reflection by blood," IEEE Transactions on Biomedical Engineering **BME-17**(2), 122 (1970).
[28] J. H. Barbee and G. R. Cokelet, "The Fahraeus effect," Microvasc Res **3**(1), 6–16 (1971).
[29] P. Gascoyne, J. Satayavivad, and M. Ruchirawat, "Microfluidic approaches to malaria detection," Acta Tropica **89**(3), 357–369 (2004).